JOURNAL OF PROPULSION AND POWER
Vol. 19, No. 4, July–August 2003

Analytical and Experimental Studies of Tile-Shaped Aerospike Nozzles

Wu-Ye Dai,* Yu Liu,† Xian-Chen Cheng,‡ and Bin Ma§
Beijing University of Aeronautics and Astronautics, 100083 Beijing, People's Republic of China

In search of an engine for space propulsive application that has higher performance and easier implementation, a new aerospike nozzle with axisymmetric thrust cells and concave plugs is studied. Numerical and experimental studies were carried out for such a nozzle with an area ratio of thrust cells of 3.24 and an overall expansion ratio of 22.15. The theoretical formulations was based on three-dimensional Reynolds-averaged Navier–Stokes equations. Turbulence closure was achieved using a low Reynolds number k–ε equation model. The companion experimental study utilized gaseous oxygen and alcohol as propellants. Results indicate that the tile-shaped plug resulted in a better flow force leading to a less restricting force-bearing condition for tile-shaped plug. For the tested model, a maximum nozzle efficiency of 0.95 near the design pressure ratio was obtained, and it has an obvious potential to increase performance by some percentage. Although the tile-shaped aerospike nozzle needs to be studied further, it is clear that it has high performance, has good altitude compensation ability, has case of implementation, and should be attractive for use in future propulsion systems.

Nomenclature

A_t	=	throat area
C_F	=	thrust coefficient
C_p	=	specific heat at constant pressure
C_v	=	specific heat at constant volume
F	=	thrust
k	=	kinetic energy of turbulence
M	=	Mach number
P	=	pressure
T	=	temperature
x, y, z	=	Cartesian coordinates
γ	=	ratio of specific heat
ε	=	turbulence dissipation rate
ε_{all}	=	overall area ratio of aerospike nozzle
ε_c	=	area ratio of a thrust cell
η	=	nozzle efficiency

Subscripts

a	=	ambient
c	=	combustion chamber
d	=	design point
i	=	ideal
p	=	primary flow
s	=	secondary flow

Introduction

CONVENTIONAL propulsive nozzles for propulsion applications, such as bell-shaped and conical nozzles, have been successfully used in rocket engines, ramjets, and turbojets for many years. The advantages of such nozzles include the availability of accurate design techniques, efficient design-point performance, and acceptable weight and cost. These nozzles, however, suffer deficiencies, such as excessive length and inefficient off-design performance, and, thus, are limited for single-stage-to-orbit(SSTO) transportation. In light of this, at least 12 nozzle concepts have been considered to overcome those disadvantages for SSTO transportation.[1,2] Among these nozzle concepts, the aerospike or plug nozzle is considered to have the best capabilities for continuous altitude compensation.[2] The aerospike nozzle also has many other advantages, such as reasonable length, uniform load distribution, and flexible structure combination. However, because of technical difficulties, the aerospike nozzle has not been applied in aeronautic or astronautic use for several decades since the concept was introduced. Nevertheless, investigations of aerospike nozzles have been undertaken because of its great prospects.

The term aerospike was initially referred to the full-length aerodynamically designed annular nozzle shown schematically in Fig. 1a. After several decades of studies, the nozzle is now generally made up of many small units, each of which consists of a thrust cell, a plug, and generally a base surface (Fig. 1b). Representative examples include the linear nozzle used in the X-33 program in the United States[3] and the clustered nozzle investigated in the Advanced Rocket Propulsion Technology (ARPT) program in Europe.[4]

In addition to the mentioned advantages, linear and clustered aerospike nozzles have other advantages. The use of clustered thrust cells allows thrust vector control of the aerospike nozzle by regulating the propellant flow rate of each unit. The servomechanism can, thus, be substantially simplified, consequently producing a much lighter engine system.

However, a linear aerospike nozzle, whose center body, that is, plug, is a large curved plate, introduces problems of an extremely high force-bearing condition and excessive weight. If the plug produced 20% thrust of an engine with the takeoff thrust of 6,000,000N, then 1,200,000 N thrust is borne by the plug, which is a very big challenge for the large plate. Furthermore, because of the effects of backpressure and freestream, the pressure distribution on the plug is uneven and varies with flight altitude, causing an even more serious force-bearing requirement of the plug. Because the plug is impacted by lateral force that keeps varying during the flight, the plug structure has to be reinforced, and consequently, the weight of the aerospike nozzle increases.[5]

The problem for the clustered aerospike nozzle concerns the flow baddistribution. On the plug, the exhaust gases of adjacent thrust cells interact with each other, which results in a quite different flowfield structure in comparison with linear aerospike nozzles. Additional shocks are induced, which influence the entire flowfield. This

Presented as paper 2002-4035 at the AIAA/ASME/SAZ/ASZE 38th Joint Propulsion Conference and Exhibit, Indianapolis, IN, 7–10 July 2002; received 27 September 2001; revision received 29 November 2002; accepted for publication 7 March 2003.

*Ph.D. Candidate, School of Astronautics.
†Professor, School of Astronautics.
‡Professor, School of Astronautics.
§Engineer, School of Astronautics.

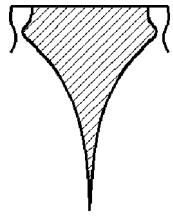

a) Full-length aerospike

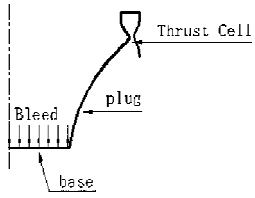

b) Aerospike unit

Fig. 1 Aerospike nozzle concepts.

nonhomogeneous flow causes additional performance loss that may rise a few percent.[6]

Common problems faced for linear and clustered aerospike nozzles are the selection and the design of the thrust cells. For a linear aerospike nozzle, because the plug is a large curved plate, the thrust cell exits are expected to be square or rectangular. If two-dimensional nozzles are employed for thrust cells, problems, such as higher heat load, cooling requirement in the throat, thermal distortion, structural warping, and nonhomogeneous flow, will be induced.[7] On the other hand, if three-dimensional nozzles are adopted, the design and manufacture of such nozzles will be more complex causing thermal distortion and performance loss.[7] For a clustered aerospike nozzle, if toroidal or linear thrust chambers are employed, the same problems as those induced for the linear aerospike nozzle by the two-dimensional nozzle arise. If a bell-shaped nozzle is used for the thrust cell, as already mentioned, the nonuniformity of the flow will be also evoked, which will lead to performance loss.[8]

This paper introduces a new aerospike nozzle, where the thrust cell is axisymmetric (such as the bell-shaped nozzle) and the plug is concave. It is called a tile-shaped aerospike nozzle because its plug looks like a tile. This nozzle can overcome the cited shortcomings to a certain extent. Numerical and experimental studies were conducted for such a nozzle.

Tile-Shaped Aerospike Nozzle Concepts

Figure 2 shows several tile-shaped aerospike nozzles, with a common feature that all the thrust cells are axisymmetric and the plugs are concave. The following are advantages of such nozzles. First, the smooth transition between thrust cells and the plug surfaces leads to a better flowfield structure on the plug surface in comparison with traditional clustered aerospike nozzles. Second, the exhaust gas of each thrust cell continues to expand, mainly in its respective plug, which may reduce the exhaust gas interaction between adjacent thrust cells. Third, the plug with concave tile-shaped structure can undertake more thrust load than that with the planar shape under the same conditions. Fourth, the thrust cell of such nozzle is axisymmetric, so that the bell-shaped nozzle can be employed. Accordingly, it can utilize the available design techniques for the bell-shaped nozzle. Fifth, the problems in thrust cells such as thermal distortion, structural warping, and non-homogeneous flow can also be improved because the bell-shaped can be employed as the thrust cell. Sixth, such a nozzle is also flexible for structure combination. For example, it may be linear, as shown in Fig. 2a, which is similar to the linear aerospike nozzle in the U.S. X-33 program, or clustered like that considered in the European ARPT program (Fig. 2b). Figure 2c shows a circular–linear configuration studied in the People's Republic of China.[9] Some studies[10,11] reveal that the performance can be improved by closing the flowfield of plug and base regions. An external form of a lifting body is considered

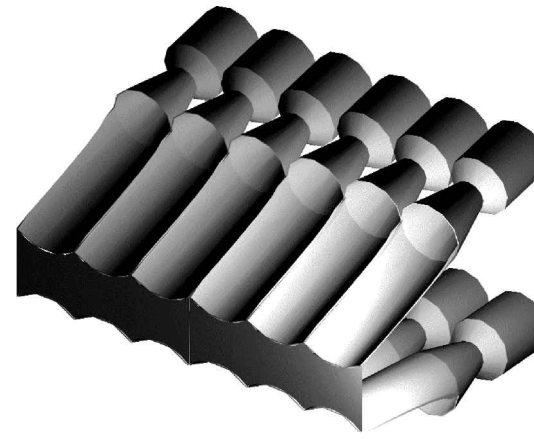

a) Linear

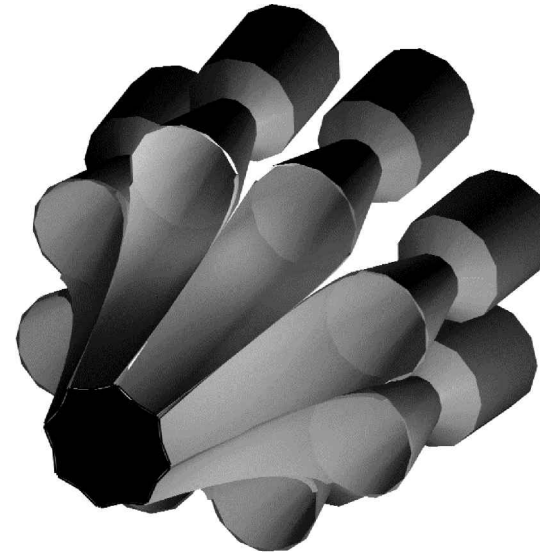

b) Circular

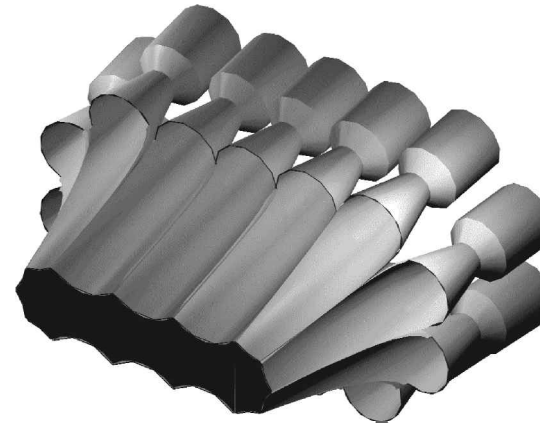

c) Circular–linear

Fig. 2 Tile-shaped aerospike nozzles.

to meet the need of SSTO. Such a circular–linear nozzle can make the flowfield of plug and base regions closed, as well as fitting the external form of lifting body. Seventh, a tile-shaped aerospike unit (including thrust cell and plug here) can be manufactured by incising a bell-shaped nozzle with a large area ratio, and consequently, the difficulty of design and manufacture of such nozzles will decrease.

On the other hand, the design and manufacture of the cooling system, as well as the assembly of each single aerospike unit for tile-shaped aerospike nozzles, are full of difficulties. A possible problem is that the divergence angle of the thrust cell may be much

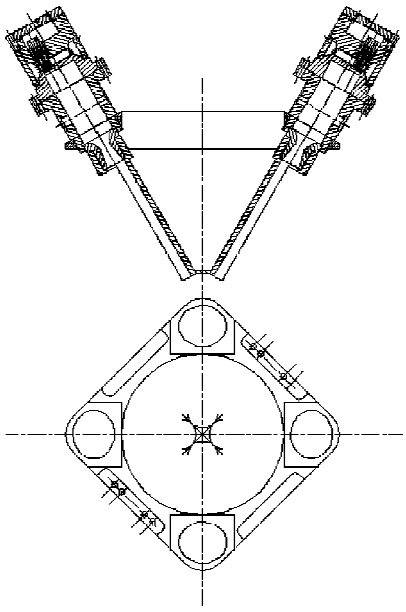

Fig. 3 Aerospike nozzle tested.

greater than zero if the aerospike unit is manufactured by incising a bell-shaped nozzle with large area ratio, and consequently, the exhaust gases of adjacent thrust cell will interact with each other, which will results in an additional performance loss.

Tested Tile-Shaped Aerospike Model

The tile-shaped aerospike nozzle investigated here is "clustered" by four units (Fig. 3). Note that the plugs are contoured by cylindrical surfaces instead of characteristic surfaces. The cylindrical plug makes the exit angle of thrust cell zero, which induces a better flowfield structure and reduces the exhaust mixing of adjacent thrust cells in comparison with that of the thrust cell with the exit angle greater than zero. The base region will also be strongly compressed by the exhaust gas departing from the plug, which results in a higher base pressure. Accordingly, the base produces larger thrust (or lower drag). At the same time, the difficulties of the design and manufacture decrease. On the other hand, also note that the cylindrical plug might induce a nonideal flowfield, which will lead to an additional performance loss.

Each thrust cell of the model studied here is a small bell-shaped nozzle as mentioned earlier. The expansion wall contour is designed by using the Rao method and is determined by an approximation of two arcs. The main parameters of the aerospike unit are shown in Fig. 4. Here $\varepsilon_c = 3.24$, and

$$\varepsilon_{\text{all}} = d_e \times h/A_t + \varepsilon_c \sin 30\ \text{deg} = 22.15 \tag{1}$$

so that the design-point nozzle pressure ratio (NPR_d) P_c/P_a, can reach about 220.

Experimental Setup

Gaseous oxygen and alcohol were adopted as propellant for the hot-gas test of the four-unit clustered tile-shaped aerospike nozzle. A complete hot-gas experimental setup was fabricated for this study (Fig. 5). The setup consists mainly of a gaseous oxygen supply system, a pressure-fed fuel ethyl alcohol supply system, a pressurized water circulating cooling system, a purging system, a high-pressure air source, a vacuum pump and two large cylindrical vacuum exhaust tanks, a cubic test vacuum room and test aerospike engines, the computer data acquisition system, and the manual controlling and monitoring system. The maximum design mass flow rate of the alcohol is 0.9 kg/s and that of the oxygen is 1.3 kg/s. Two venturi tubes used to adjust the flow rate are mounted in the oxygen line and the alcohol line, respectively. The design combustion chamber

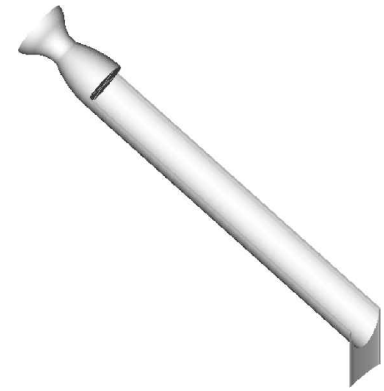

a) Three-dimensional perspective view

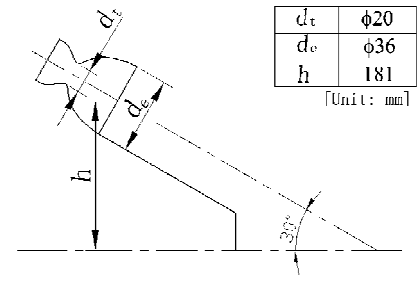

b) Longitude plane

Fig. 4 Aerospike unit and its main parameters.

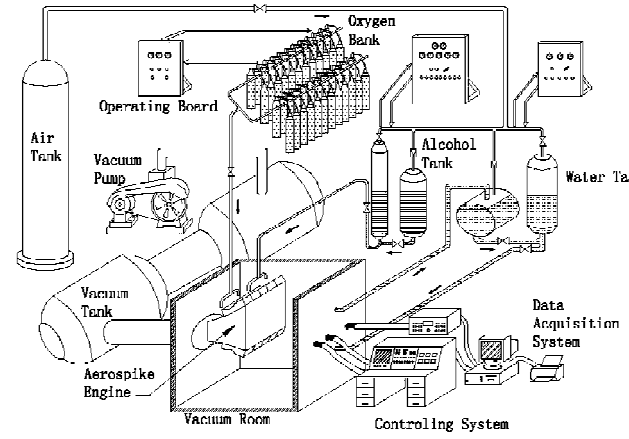

Fig. 5 Hot-gas test system.

pressure for the system reaches 5 MPa, although the real pressure of the current hot-gas test was about 1.7 MPa.

Among all of the measured parameters, the thrust and combustion chamber pressure are most important for the performance understanding of the tested model. The thrust testing rack is installed horizontally in the cubic test room. To maintain automatically its thrust force line accurately, a special device was designed, which converts the thrust to a pulling force. The thrust testing rack can reach the precision required, and root-mean-square error analyses reveals that the uncertainty of the entire thrust acquisition is less than 1%. The acquisition of combustion chamber pressure is simpler and more accurate than that of thrust. When modern sputtered film-type pressure transducers are used, the uncertainty of pressure acquisition is less than 0.5% in the present system.

Numerical Method

Governing Equations and Discretization

The flow is modeled by the compressible three-dimensional conservation equations of Reynolds-averaged Navier-Stokes (N–S) equations. It is assumed in the current study that the specific heats

c_p and c_v and, consequently, γ may be considered constant with reasonable accuracy. The values of the Reynolds stresses and turbulent heat fluxes, which are necessary for N–S equations, are obtained using the Lam–Bremhost k–ε turbulence model.[12]

The second-order nonoscillatory and non-free-parameters dissipative finite difference scheme (NND scheme)[13] was employed for the discrete convective terms, and second-order central differencing scheme is used for viscous terms. This NND scheme has been adopted to for many complex flow simulations[11,14] and it is valid to solve aerospike nozzle flow.

The N–S equations and k–ε model equations were solved iteratively in the present work, and the same solving procedure was adopted due to their similar forms. An implicit two-step procedure can be obtained by applying the hybrid flux-splitting method to N–S equations and k–ε model equations, respectively.[14] This two-step procedure has good stability, and the system of differential equations is in tridiagonal form, which can be solved very efficiently using standard Gaussian two-step elimination procedure.

Boundary Conditions

Because of the symmetry of plug flow, the computations were done only at a half-domain of an aerospike nozzle unit. Because the expansion ratio of the thrust cell is small, the effect of backpressure on the flow in the thrust cell can be neglected; therefore, the calculations of the internal flow for the thrust cell and the external flow for the plug were done separately. The flow parameters of the exit of the thrust cell were used as an inflow boundary condition for the plug flow. The calculations and the results of the internal flow of the thrust cell are not given here in detail.

The boundary conditions used for the N–S equations generally contain inflow condition, no-slip wall and adiabatic wall conditions, outflow conditions, and symmetry condition.[15] Besides those, the boundary conditions for the plug flow also include a far-field boundary for the freestream, where the Riemann condition was used. The inflow of plug flow was fixed by the results obtained by thrust cell computation.

The boundary conditions used for the k–ε equations are quite simple. The values of k and ε are extrapolated at the outflow boundary and symmetry plane. Both k and ε are set to zero on the solid wall, and k and ε are imposed at the inflow boundary as follows[15,16]:

$$k = 0.0006u^2 \tag{2}$$

$$\varepsilon = C_u^{3/4} k^{1.5} / L \tag{3}$$

where C_u is a constant equal to 0.09, u is the inflow velocity, and

$$L = \min\{0.085\delta, 0.4y^+\} \tag{4}$$

where δ is the boundary thickness and y^+ is the vertical distance to the wall.

To ensure the stability of the computational procedure, the limiters for k and ε presented in Ref. 15 are employed in the current method.

Computational Strategy

Some complicated physical phenomena, such as shocks, expansion waves, compressive waves, vortices and flow separations, may appear in aerospike nozzle flow, especially when simulating the flow at low altitude. Accordingly, difficulty to simulate the aerospike flow effectively can be expected. To accelerate the convergence rate and to ensure the stability of the computational procedure, the numerical simulation was first run with a coarse grid of $36 \times 33 \times 13$ and Courant–Friedrichs–Lewy number (CFL) = 30. Based on the results of the coarse grid, the solution procedure was done with a fine grid of $71 \times 65 \times 25$ and CFL = 120. Last, the computation was continued with the fine grid and CFL = 20 until the solution met the required precision.

Results and Analysis

Flowfield Simulation

The thrust chamber conditions were specified according to the tests, with $P_c = 1.7$ MPa and $T_c = 1500$ K. Figure 6 shows the plug model. Note that there is a flat step connecting the tile-shaped plug with 2 mm width. The flat step is the joint of the two adjacent units. The Mach number distribution at the thrust cell exit is also shown in Fig. 6. All of the following results of plug flow were obtained based on this result.

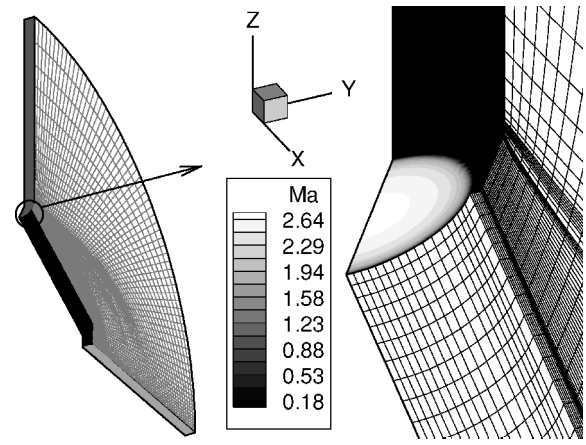

Fig. 6 Plug model and Mach number distribution of thrust cell exit.

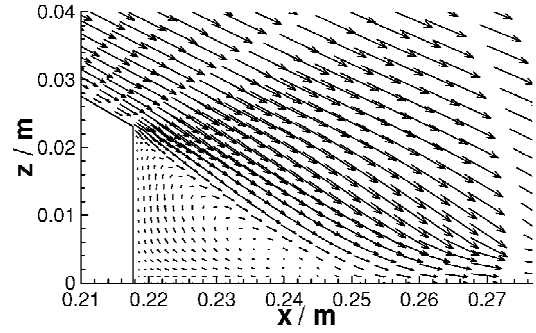

Fig. 7 Vector distribution around the base at center plane, NPR = 220.

Figure 7 presents the velocity vector distribution around the base at the center plane, namely, $y = 0$ plane, for the case NPR = 220. A subsonic vortex appears in the base, which is an important characteristic of such a flow. Figure 8 shows the Mach number distributions at the center plane for NPR = 220 and 17, respectively, and at the side plane, namely, $y = y_{\max}$, the plane where the unit connects to another unit, for NPR = 17. The base flow is attached, and a trailing shock rises for NPR = 220. Nevertheless, at NPR = 17, the freejet flow boundary is strongly compressed by the ambient gas and the exhaust gas of the thrust cell flow along the plug. Note that no flow separation arises even at NPR = 17 and that there are some distinct differences between the flow at the center and side planes.

Figure 9 shows the plug wall pressure distributions at the center and side planes at NPR = 17 and 220. The pressure profiles at the center plane are different from that at the side plane, especially when x is less than 0.06 m, and the trend of the presented results is similar to the experimental results in Ref. 10. It is found that at low altitude, the pressure at the side plane, where one aerospike unit connects to another, fluctuates around ambient pressure, so that the joint of two adjacent units also offers some thrust or only a little drag. At high altitude, the pressure at the side plane is similar to that at the center plane after the point $x = 0.07$ m, whereas upstream of that point the side pressure is a little lower than the center pressure due to the effect of the flat step connecting another unit. However, the side pressure is still much higher than backpressure. Thus, thrust is produced both at the center plane and at the side plane.

To study the plug flow further, a numerical simulation was undertaken on a model where the plug surface was planar instead of tile-shaped and all of the other structure parameters and working parameters were fixed as the same as those of this tile-shaped aerospike. The result of the plug wall pressure distributions of the

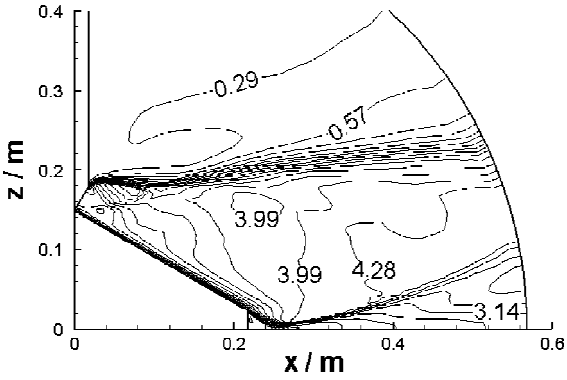

a) At center plane, NPR = 220

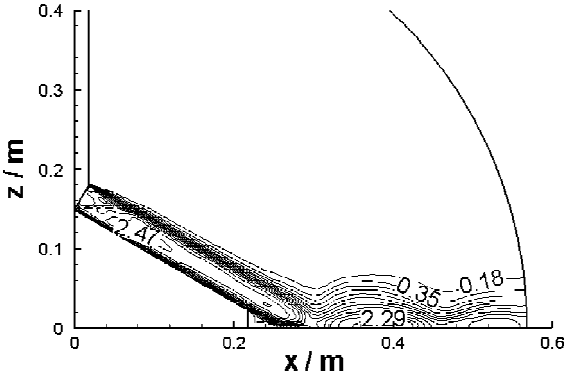

b) At center plane, NPR = 17

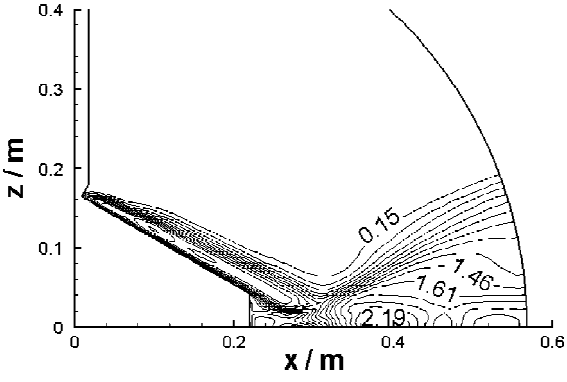

c) At side plane, NPR = 17

Fig. 8 Mach number distributions.

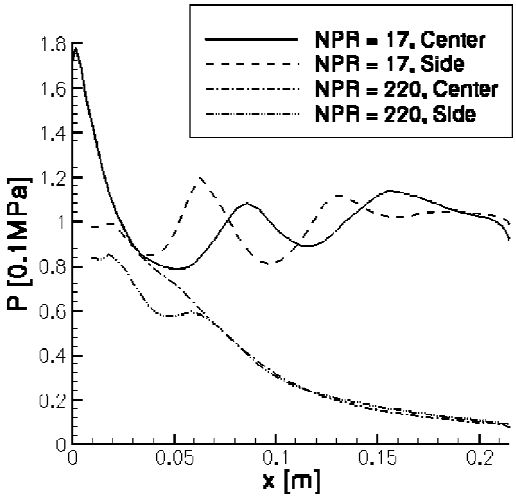

Fig. 9 Plug wall pressure profiles of tile-shaped plug.

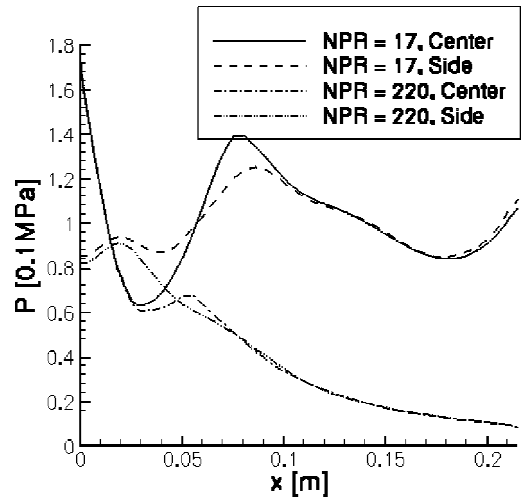

Fig. 10 Plug wall pressure profiles of planar plug.

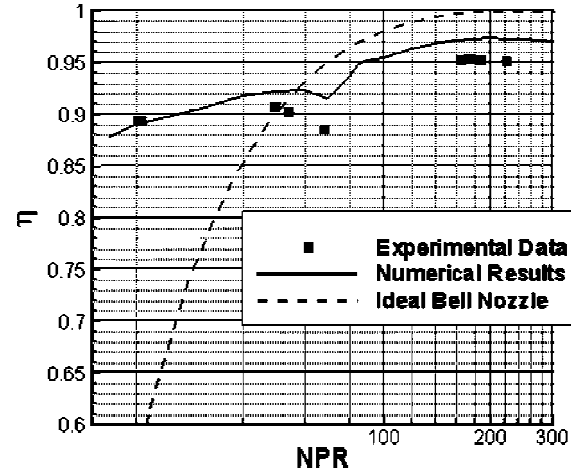

Fig. 11 Variation of nozzle efficiency of tile-shaped nozzle as a function of NPR.

modified model is shown in Fig. 10. When Figs. 9 and 10 are compared, it is found that the range of pressure on the tile-shaped plug wall is small in comparison with that on the planar plug. As a result, the tile-shaped plug is impacted by a relatively smaller force, leading to a less restricting force-bearing condition for the tile-shaped plug.

Although some numerical results should be further validated by experiments, it is clear that the tile-shaped plug will induce better flow than the traditional plug and, thus, will promote performance.

Nozzle Efficiency

Here, η is defined as $\eta = C_F/C_{F_i}$, where $C_F = F/P_c A_t$ is the thrust coefficient from experimental or numerical results and C_{Fi} is

$$C_{F_i} = \sqrt{\gamma}[2/(\gamma+1)]^{[(\gamma+1)/2(\gamma-1)]} \times \sqrt{2\gamma/(\gamma-1)[1-(1/\mathrm{NPR})^{(\gamma-1)/\gamma}]} \tag{5}$$

The variation of η is plotted as a function of NPR in Fig. 11. The dashed line denotes the one-dimensional theoretical η for the bell-shaped nozzle with the same expansion ratio without any loss, namely, C_{Fi} is obtained using Eq. (5), whereas C_F is calculated by

$$C_F = \sqrt{\gamma}[2/(\gamma+1)]^{[(\gamma+1)/2(\gamma-1)]} \times \sqrt{2\gamma/(\gamma-1)[1-(1/\mathrm{NPR}_d)^{(\gamma-1)/\gamma}]} + \varepsilon_{\mathrm{all}}[(1/\mathrm{NPR}_d)-(1/\mathrm{NPR})] \tag{6}$$

The results reveal that the numerical results are a little higher than the experimental results, but their trends are very similar. The

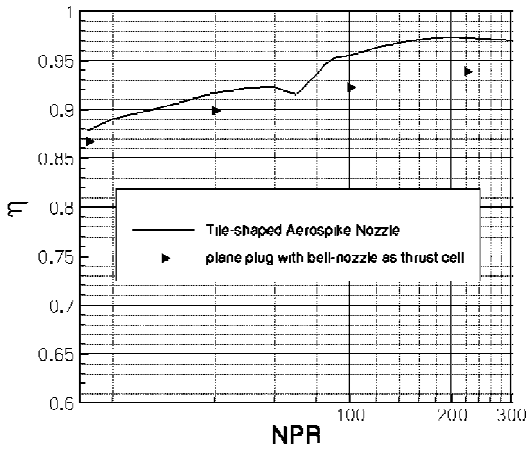

Fig. 12 Performance comparison between tile-shaped nozzle and planar plug nozzle (predictive).

experimental maximum of η is about 0.955 around NPR = 220. The aerospike nozzle has better altitude compensation ability than the bell-shaped nozzle: The η of the aerospike nozzle is higher than that of the ideal bell-shaped nozzle at NPR < 75, and it varies from 0.89 to 0.95 with the change of flight altitude from the ground to the design altitude (NPR = 16.8 ~ 220). The trend of the presented results is similar to that in the published literature.[17,18]

The predictive results of the tile-shaped and the planar plug nozzles are shown in Fig. 12. The result shows that the model with planar plug has the worse performance and the loss of performance rises up to 3%. This means tile-shaped plug nozzles have a better performance at the same conditions. However, this result should be validated further by experiments.

although the tile-shaped aerospike nozzle has good altitude compensation ability, as analyzed earlier, the experimental maximum of η of this tested model is about 2% lower than that of the models presented in the literature.[17,18] The reasons are very clear. First, the model tested here has only four units. Strictly speaking, it is not a real clustered nozzle, so that the performance loss should be obvious. A second reason, the main reason, is that the plug surface of the current model is cylindrical, and consequently, the performance of this model should be lower than that of the model employing characteristic plug surfaces. This can be understood because the performance of a conical nozzle with a divergent half-angle of 15-deg is a few percent lower than that of a bell-shaped nozzle under the same conditions. Third, the present thrust cell was contoured by an approximation of two arcs, which may result in an additional performance loss. Last, the tested model in Ref. 18 is a full-length aerospike nozzle; thus, its performance should be higher than a truncated aerospike nozzle. Therefore, if the presented model is perfected, the performance of such tile-shaped aerospike nozzle should increase by some percentage. Thus, a tile-shaped aerospike nozzle such as that introduced in this paper can be expected to have performance as good as, if not better than, traditional linear or clustered aerospike nozzles. If the advantages of such nozzle analyzed earlier are taken into account, the tile-shaped aerospike nozzle should be more attractive for use in future propulsion systems.

Conclusions

A tile-shaped aerospike nozzle with axisymmetric thrust cells and concave plugs is introduced. Numerical and experimental studies were carried out for the model with the thrust cell aeroratio of 3.24 and the overall expansion ratio of 22.15. Such a nozzle leads to a less restricting force-bearing condition for a tile-shaped plug. The experimental results indicate that the maximum η of the presented model is more than 0.95 and that η varies from 0.89 to 0.95 with change of flight altitude from ground to the design altitude. If the design of this aerospike nozzle is perfected, (the thrust cells and the plugs, for instance, are contoured by characteristic faces), the performance can be improved further. In addition, there are some distinct advantages of such nozzles, such as that the plug with concave tile-shaped structure can bear more thrust load than that with a planar one under the same conditions, that it has a flexible structural combination, and that design and manufacture techniques are already available. Further more, the nozzle can improve some problems in thrust cells, including thermal distortion, structural warping, nonhomogeneous flow, and so forth. Although this aerospike nozzle needs to be studied further, it is obvious that it has high performance, especially good altitude compensation ability, and that it is easy to implement. The tile-shaped aerospike nozzle should be considered attractive for use in the future propulsion systems.

References

[1]Beichel, R., "Nozzle Concepts for Single-Stage Shuttles," *Astronautics and Aeronautics*, Vol. 13, No. 6, June 1975, pp. 16–27.

[2]Muss, J. A., and Nguyen, T. V., "Evaluation of Altitude Compensating Nozzle Concepts for RLV," AIAA Paper 97-3222, July 1997.

[3]Bokullich, F., "X-33 Advanced Technology Demonstrator Scheduled to Fly in 1999," *Aerospace America*, Vol. 18, No. 3, March 1998, p. 18.

[4]Vuilamy, D., Duthoit, V., and Berry, W., "European Investigation of Clustered Plug Nozzles," AIAA Paper 99-2350, June 1999.

[5]Dai, W.-Y., Liu, Y., Cheng, X.-C., and Tang, H.-B., "Aerospike Nozzle Performance Study and Its Contour Optimization," AIAA Paper 2001-3237, July 2001.

[6]Hagemann, G., Immich, H., and Terhardt, M., "Flow Phenomena in Advanced Rocket Nozzles—the Plug Nozzle," AIAA Paper 98-3522, July 1998.

[7]Booth, T. E., Vilja, J. O., Cap, D. P., and McGill, R. J., "The Design of Linear Aerospike Thrust Cells," AIAA Paper 93-2562, June 1993.

[8]Fick, M., and Schmucher, R. H., "Performance Aspects of Cluster Nozzles," *Journal of Spacecraft and Rockets*, Vol. 33, No. 4, 1996, pp. 507–512.

[9]Liu, Y., Zhang, G.-Z., Dai, W.-Y., Ma, B., Cheng, X.-C., Wang, Y.-B., Qin, L.-Z., Wang, C.-H., and Li, J.-W., "Experimental Investigation on Aerospike Nozzle with Different Structures and Working Conditions," AIAA Paper 2001-3704, July 2001.

[10]Tomita, T., Takahashi, M., Ododera, T., and Tamura, H., "Effects of Base Bleed on Thrust Performance of a Linear Aerospike Nozzle," AIAA Paper 99-2586, June 1999.

[11]Li, J., "Study on Gas Dynamic Process of Aerospike Nozzle, Measurements of Hypersonic Dynamic Stability Derivatives of Space Shuttles," Postdoctoral Dissertation, Inst. of Mechanics, Chinese Academy of Sciences, Beijing, June 2001 (in Chinese).

[12]Lam, C. K. G., and Bremhorst, K. A., "Modified Form of the k–ε Model for Predicting Wall Turbulence," *Journal of Fluids Engineering*, Vol. 103, No. 3, Sept. 1981, pp. 456–460.

[13]Zhang, H.-X., "Non-Oscillatory and Non-Free-Parameter Dissipation Difference Scheme," *ACTA Aerodynamica Sinica*, Vol. 6, No. 2, 1988, pp. 143–165, (in Chinese).

[14]Cheng, J.-Q., "Numerical Simulations on Supersonic Combustion Flow and Swirl Flow," Ph.D. Dissertation, Researching and Developing Inst. of Chinese Aero-power, Sichuan, People's Republic of China, Dec. 1995.

[15]Gerolymos, G. A., and Vallet, I., "Implicit Computation of Three-Dimensional Compressible Navier–Stokes Equations Using k–ε Closure," *AIAA Journal*, Vol. 34, No. 7, 1996, pp. 1321–1330.

[16]Xu, X., "Numerical Simulation of Nozzle Flow for Liquid Rocket Engine with Mass Injection," Ph.D. Dissertation, Dept. of Power, Beijing Univ. of Aeronautics and Astronautics, Beijing, Nov. 1997.

[17]Silver, R., "Advanced Aerodynamic Spike Configurations: Volume 1, Analytical and Cold Flow Studies," Rocketdyne Div., Rept. AFRPL-TR-67-246-Vol I, Air Force Contract 04(611)-9948, Rockwell International Corp., Sept. 1967.

[18]Tomita, T., Takahashi, M., and Onodera, T., "Visualization of Shock Wave Interaction on the Surface of Clustered Plug Nozzles," AIAA Paper 98-3523, July 1998.